Available online at www.sciencedirect.com

ScienceDirect

Journal of the Franklin Institute 359 (2022) 9110–9128

www.elsevier.com/locate/jfranklin

Numerically efficient H_∞ analysis of cooperative multi-agent systems☆

Ivica Nakić[a], Domagoj Tolić[b,*], Zoran Tomljanović[c], Ivana Palunko[d]

[a] *Department of Mathematics, Faculty of Sciences, University of Zagreb, Zagreb, Croatia*
[b] *LARIAT – Laboratory for Intelligent Autonomous Systems & RIT Croatia, Dubrovnik, Croatia*
[c] *Department of Mathematics, J. J. Strossmayer University of Osijek, Osijek, Croatia*
[d] *LARIAT – Laboratory for Intelligent Autonomous Systems, University of Dubrovnik, Croatia*

Received 9 April 2022; received in revised form 24 July 2022; accepted 17 September 2022
Available online 26 September 2022

Abstract

This article proposes a numerically efficient approach for computing the maximal (or minimal) impact one agent has on the cooperative system it belongs to. For example, if one is able to disturb/bolster merely one agent in order to maximally disturb/bolster the entire team, which agent to choose? We quantify the agent-to-system impact in terms of H_∞ norm whereas output synchronization is taken as the underlying cooperative control scheme. The agent dynamics are homogeneous, second order and linear whilst communication graphs are weighted and undirected. We devise simple sufficient conditions on agent dynamics, topology and output synchronization parameters rendering all agent-to-system H_∞ norms to attain their maxima in the origin (that is, when constant disturbances are applied). Essentially, we quickly identify bottlenecks and weak/strong spots in multi-agent systems without resorting to intense computations, which becomes even more important as the number of agents grows. Our analyses also provide directions towards improving communication graph design and tuning/selecting coopera-

☆ This work was supported in part by Croatian Science Foundation under the projects IP-2016-06-2468 (ConDyS) and IP-2019-04-6774 (VIMS), in part by SeaClear, European Union's Horizon 2020 research and innovation programme under grant agreement No. 871295, and in part by the European Regional Development Fund under the grant KK.01.1.1.01.0009 (DATACROSS).

* Corresponding author.
E-mail address: domagoj.tolic@croatia.rit.edu (D. Tolić).

https://doi.org/10.1016/j.jfranklin.2022.09.013

tive control mechanisms. Lastly, numerical examples with a large number of agents and experimental verification employing off-the-shelf nano quadrotors are provided.

1. Introduction

The network topology and agent dynamics play crucial roles in Multi-Agent System (MAS) stability and performance [1,2]. Even in networks of homogeneous agents, not all agents have the same impact on other agents or joint performance depending on their location within the underlying topology. Taking this observation into account, we tackle the following question: *Given some topology, if one is to disturb (or bolster) one or more agents in order to undermine (or enhance) the performance of the entire team, which agent(s) to choose?* Similarly, various topologies interconnecting the same group of agents typically result in strikingly different collective behaviors and even in the lack thereof. Consequently, the system designer might want to *modify the graph edge weights, remove or add communication/sensing links in an effort to preclude unfavorable cooperative behaviors*. Over last decades, similar analyses are routinely carried out for vibrational systems (e.g., buildings, bridges, etc.), which can be modeled as MASs [3–5]. Vibrations are typical and mostly unwanted phenomenon in mechanical systems, since resonance and sustained oscillations can have undesired effects such as energy waste, noise creation and even structural damage. Similar ideas are also found in social networks, economics, political and health care systems (e.g., sociometric stars, invisible colleges, outsiders or cliques [6–9]) as well as in smart grids [10,11]. In other words, the aforementioned communication, sensing and social networks, vibrational, mechanical, economic, political and health care systems as well as smart grids are examples of application domains for this work.

In this work, we investigate how to efficiently calculate the H_∞ norm of MASs when one agent is disturbed. The main idea is to reduce the problem from the order $2n\times 2n$ to the order $(n-1)\times(n-1)$ and to cast the problem of H_∞ norm calculation into solving a sequence of linear systems. Then we show that, for a large class of MASs, the transfer function attains its maximum at the origin (that is, when the disturbance is constant), thus reducing the computation of H_∞ norm to solving just a single linear system. These two components greatly reduce the computation time enabling efficient investigations of very large MASs. Computational costs behind finding H_∞ norms are at times quite high even for systems of moderate sizes, not to mention when various system parameters or input-output pairs need to be considered. Therefore, efficient calculations of the H_∞ norm are intensively investigated, especially when a large number of agents/states is encountered [12–18].

Topology discovery is often the first step in bottleneck and failure identification of MASs. Early decentralized topology discovery algorithms are reported in [19,20] whereas there are many commercial solutions available nowadays (which will not be advertise here). Owing to the availability of such algorithms, this work supposes that the topology is provided a priori.

Works relating the H_∞ norm and MASs typically focus on syntheses (see [21–25] and references therein) whilst our article is primarily concerned with analyses. For exam-

ple, [21,22] boil down to Linear Matrix Inequalities (LMIs) whereas [23] builds upon game theory and dynamic programming to provide sufficient conditions for controller design yielding MAS synchronization with a prescribed $\mathcal{L}_2$-gain. The authors in [24] provide sufficient and necessary conditions for decentralized H_∞ and H_2 control design over directed graphs employing the algebraic Riccati equation (ARE) or direct eigenstructure assignment. Even though it also focuses on syntheses, the most similar article to ours is [25] as it performs system reduction to mitigate the H_∞-related computational burden and searches for performance bottlenecks on the individual agent level. Therefore, unlike in the present work, the team performance improvement guidelines in [25] boil down merely to individual agent modifications via pinning control (i.e., via adding self-loops) irrespective of the topology. In addition, [25] considers merely stability around the origin (not around the equilibrium manifold as done herein) and does not tackle H_∞ norm computations. The H_2 norm as the MAS performance measure will be treated in a subsequent publication.

Other related cooperative control problems, other than the output synchronization considered herein, are found in [26–32]. The work in [26] synthesizes a control mechanism to attain MAS consensus about the origin in the presence of additive perturbations with a known H_∞ bound when modelling agent uncertainties. The authors in [27] synthesize observer-based controllers to track a leader, which leads to the absence of non-trivial consensus manifold encountered herein. The problem in [28] exploits the Lyapunov characterization of H_∞ control to synthesize controllers with precompensators resulting in a MAS with the sole equilibrium point in the origin. A containment problem is investigated in [29], finite-horizon problem in [30], event-based leader-follower MASs in [31] whilst event-triggered sliding mode scaled consensus control is investigated in [32]. Lastly, owing to the employment of the bounded real lemma, Lyapunov and dissipative H_∞ characterizations, none of the above works conveys information regarding which input to which agent yields the maximum/minimum MAS H_∞ norm. On the other hand, our work explicitly provides these information.

The principal contributions of this article are threefold: a) numerically efficient calculations of H_∞ norms in MASs by reducing the original $2n\times 2n$-dimensional problem into an $(n-1)\times(n-1)$-dimensional one; b) sufficient conditions for attaining the H_∞ norm in zero, thus further reducing the computational costs; and c) an experimental verification employing an affordable off-the-shelf localization system and nano quadrotors as MAS agents.

Since many MASs are designed to achieve asymptotic (i.e., steady-state) goals (e.g., output synchronization), it is not surprising they behave like low-pass filters so that the moduli of associated transfer functions attain their maxima at the zero frequency corresponding to the H_∞ norms. If one is also interested in the transient behavior (in addition to the steady-state performance), our analyses can be combined with [33] during the control design phase.

The remainder of the article is organized as follows. Section 2 introduces the notation and basic definitions. In Section 3, we set the agent-to-system impact problem up and propose the methodology to solve this problem in Section 4. Section 4 also contains the main result. In Section 5, we provide numerical examples. Section 6 presents experimental results whilst conclusions and future work are in Section 7.

2. Preliminaries

2.1. Notation

We often use the shorthand notation $(x, y) := [x^\top \quad y^\top]^\top$. The dimension of a vector x is n_x whereas $\|\cdot\|$ denotes the Euclidean norm of a vector. If the argument of $\|\cdot\|$ is a matrix, then it denotes the induced matrix 2-norm. The kernel of a matrix A is $\mathrm{Ker}(A)$. The set cardinality is denoted by $|\cdot|$. An n-dimensional vector with all entries 0 is denoted by $\mathbf{0}_n$. The $n \times n$ identity matrix is I_n. For $i \in \mathbb{N}$, by e_i we denote the ith canonical vector, i.e., the vector of the form $(0, \ldots, 0, 1, 0, \ldots, 0)$, where the only non-zero element is the ith one. For brevity, we use "w.r.t." instead of "with respect to".

2.2. Graph theory

An *undirected weighted graph* is a triple $\mathcal{G} = (\mathcal{V}, \mathcal{E}, \{w_{jk}\}_{j,k=1}^N)$, where $\mathcal{V} = \{v_1, \ldots, v_N\}$ is a nonempty set of *nodes*, $\mathcal{E} \subset \mathcal{V} \times \mathcal{V}$ is the set of *edges* and $w_{jk} \geq 0$ are edge weights, where we assume that $w_{jk} = w_{kj}$ for all j, k and that $w_{jk} > 0$ if and only if $(j, k) \in \mathcal{E}$. When the edge (i, j), $i \neq j$ belongs to $\mathcal{E}$, it means that there are information flows from the node i to the node j. The set of indices of *neighbors* of the node v_i is $\mathcal{N}_i = \{j : (v_j, v_i) \in \mathcal{E}\}$. The corresponding graph Laplacian matrix $L \in \mathbb{R}^{|\mathcal{V}| \times |\mathcal{V}|}$ is defined as

$$L = [l_{ij}], \quad l_{ij} = \begin{cases} -w_{ij}, & j \in \mathcal{N}_i, \\ \sum_{k \in \mathcal{N}_i} w_{ik}, & j = i, \\ 0, & \text{otherwise.} \end{cases}$$

Note that the matrix L is symmetric and positive semi-definite.

2.3. H_∞ norm

We define the function space $\mathcal{H}_\infty$, see, e.g., [34], by

$$\mathcal{H}_\infty = \left\{ F : \mathbb{C}^+ \to \mathbb{C}^{m \times \ell} \;\middle|\; F \text{ is analytic and } \sup_{\lambda \in \mathbb{C}^+} \overline{\sigma}(F(\lambda)) < \infty \right\}.$$

Here, $\mathbb{C}^+ = \{\lambda \in \mathbb{C} \mid \Re(\lambda) > 0\}$ and $\overline{\sigma}(T)$ is the largest singular value of the matrix T. The H_∞ norm for the functions in $\mathcal{H}_\infty$ is defined as [12], Chap. 3

$$\|F\|_\infty = \sup_{\lambda \in \mathbb{C}^+} \overline{\sigma}(F(\lambda)) = \sup_{\omega \in \mathbb{R}} \overline{\sigma}(F(\mathrm{i}\omega)).$$

3. Problem statement

Consider MAS consisting of n linear agents given by

$$\ddot{\chi}_k = -T_s \dot{\chi}_k + K_s u_k + \omega_k, \quad T_s, K_s > 0, \tag{1}$$

where χ_k is the state, u_k is the control input, and ω_k is the exogenous disturbance of the kth agent, $k \in \{1, \ldots, n\}$.

Let G be an undirected weighted graph which describes the underlying communication structure of the MAS. A widely utilized decentralized output-feedback policy to achieve

network synchronization [1,35] is

$$u_k = -K\hat{C}\sum_{j\in\mathcal{N}_i} w_{kj}\left(\begin{bmatrix}\chi_k\\ \dot{\chi}_k\end{bmatrix} - \begin{bmatrix}\chi_j\\ \dot{\chi}_j\end{bmatrix}\right), \tag{2}$$

where $K > 0$ and $\hat{C} = [c_1 \quad c_2]$ with $c_1, c_2 > 0$. According to Ren and Beard [1], if $c_1 = 0$ or $c_2 = 0$, the output synchronization is not obtainable. Utilizing the Laplacian matrix L of the underlying communication graph $\mathcal{G}$, the closed-loop dynamics are

$$\ddot{\chi} + \left(\underbrace{T_s}_{:=\beta} I_N + L\underbrace{K_s K c_2}_{:=\alpha}\right)\dot{\chi} + L\underbrace{K_s K c_1}_{:=\gamma}\chi = \omega, \tag{3}$$

where $\chi := (\chi_1, \ldots, \chi_n)$ and $\omega := (\omega_1, \ldots, \omega_n)$.

Clearly, the agent dynamics Eq. (1) represent a realistic double integrator. These dynamics allow for more specific results in the upcoming sections while still being general enough owing to the following well-known fact: for fully actuated mechanical systems a simple change of control variable transforms their dynamics into a double integrator [1]. Similarly, many systems with low-level controllers can be approximated with second order dynamics (refer to Section 6 below).

Assumption 1. We assume that the graph G is connected.

If the graph of the system is not connected, with $k > 1$ number of components, then the corresponding MAS can be split into k MASs that can be analyzed independently.

The control law Eq. (2) primarily seeks for agreement/consensus, irrespective where that agreement is obtained. Consequently, the closed-loop system Eq. (3) is characterized with the equilibrium manifold $\chi_1 = \ldots = \chi_n$, $\dot{\chi}_1 = \ldots = \dot{\chi}_n = 0$, rather than with a sole equilibrium point (in the origin, for instance). Hence, attention needs to be paid to the existence of the consensus manifold as shown in [36] and the remainder of this article. In a nutshell, the (output) norms need to be taken w.r.t. sets, rather than w.r.t. points as is typically done. In addition, the only natural way of stating our main problem of interest is in terms of norms w.r.t. sets, which is also corroborated by Section 6 in light of the problem built-in robustness. Throughout this article, the w.r.t. set notion is noticeable whenever handling the zero eigenvalue of L and associated eigenspace.

We are now ready to state the main problem solved herein.

Problem 1. Efficiently calculate the H_∞ norm of system Eq. (3) from ω_i to χ w.r.t. consensus manifold for any $i \in \{1, \ldots, n\}$ of interest.

4. Methodology

4.1. Closed-Loop dynamics reduction and transfer function formula

Let us tackle Problem 1, i.e., let us efficiently calculate the H_∞ norm of the system Eq. (3) when all ω_k, $k = 1, \ldots, n$ are zero except the ith one. This problem boils down to, see [37,38], the calculation of H_∞ norm of the following linear time-invariant system

$$\dot{x} = Ax + B_i\omega_i,$$
$$y = Cx,$$

where $x := (\chi, \dot{\chi})$ while the system matrices $A \in \mathbb{R}^{2n\times 2n}$, $B_i \in \mathbb{R}^{2n\times 1}$ and $C \in \mathbb{R}^{n\times 2n}$ are given by

$$A = \begin{bmatrix} \mathbf{0}_{n\times n} & I_n \\ -\gamma L & -\beta I_n - \alpha L \end{bmatrix}, \quad \alpha, \beta, \gamma > 0,$$
$$B_i = \begin{bmatrix} \mathbf{0}_{n\times 1} \\ e_i \end{bmatrix}, \quad C = \begin{bmatrix} I_n & \mathbf{0}_n \end{bmatrix}. \tag{4}$$

From the construction of L and Assumption 1, one knows that the algebraic multiplicity of its zero eigenvalue is one. As discussed in [35] and [1], the corresponding eigenvector is $[1, 1, \ldots, 1]^\top$. However, the corresponding transfer function

$$C(\mathrm{i}s - A)^{-1}B_i$$

does not belong to the space $\mathcal{H}_\infty$. The issue is that the transfer function is not defined in zero owing to the eigenvalue placed in the origin. This property is found in many control systems, especially in consensus-based cooperative systems [36]. Namely, such control systems primarily aim for relative (not absolute) agreement/alignment giving rise to a consensus manifold, rather than to a sole equilibrium point. For instance, formation control is concerned with formation attainment irrespective of the formation absolute location.

To remove the absolute values of consensus/agreement points and concentrate on relative discrepancies among agents' outputs, let us define the following truncation matrix

$$W^\top = \begin{bmatrix} V^\top & 0 \\ 0 & I \end{bmatrix} \in \mathbb{R}^{(2n-1)\times 2n} \tag{5}$$

with orthonormal columns, where the columns of matrix $V \in \mathbb{R}^{n\times(n-1)}$ span the subspace $\{\mathbf{1}\}^\perp$ where $\mathbf{1} = [1 \ \ldots \ 1]^\top$ and such that $V^\top V = I$.

Now, by using the substitution $x = W\tilde{x}$, the reduced system is given by

$$\dot{\tilde{x}} = \tilde{A}\tilde{x} + \tilde{B}_i\omega_i,$$
$$y = \tilde{C}\tilde{x},$$

with $\tilde{A} = W^\top AW$, $\tilde{B}_i = W^\top B_i$ and $\tilde{C} = CW$. Moreover, using the block structure of matrices given by Eq. (5) and Eq. (4), we have that

$$\tilde{A} = \begin{bmatrix} 0 & V^\top \\ -\gamma LV & -\beta I - \alpha L \end{bmatrix},$$
$$\tilde{B}_i = \begin{bmatrix} 0 \\ e_i \end{bmatrix}, \quad \tilde{C} = \begin{bmatrix} V & 0 \end{bmatrix}.$$

The obtained reduced system has the property that the state matrix $\tilde{A}$ is Hurwitz and moreover models the dynamic of MAS with respect to the relative distance between the agents. An alternative (and more common) approach is to consider all the differences between the states of neighbors as the MAS state (see [1,39] or practically any of the references herein). Note that our approach yields a much smaller dimension of the system since the approach from Ren and Beard [1], Kingston et al. [39] potentially yields the dimension $4n^2 - 2n$ of the state vector whilst the dimension of the state vector is $2n - 1$ in our approach.

In order to obtain an explicit formula for the transfer function $F_i(s) = \tilde{C}(sI - \tilde{A})^{-1}\tilde{B}_i$ of the reduced system, we first obtain for $s \neq 0$ that

$$(\mathrm{i}s - \tilde{A})^{-1} = \begin{bmatrix} V^\top\Phi(s)^{-1}(\mathrm{i}sI + \beta I + \alpha L)V & V^\top\Phi(s)^{-1} \\ -\gamma\Phi(s)^{-1}LV & \mathrm{i}s\Phi(s)^{-1} \end{bmatrix}, \tag{6}$$

where

$$\Phi(s) = -s^2 I + \mathrm{i}s(\beta I + \alpha L) + \gamma L V V^\top. \tag{7}$$

Hence, the transfer function of the reduced system is given by

$$\begin{aligned} F_i(s) &= \tilde{C}\left(\mathrm{i}sI - \tilde{A}\right)^{-1}\tilde{B}_i \\ &= VV^\top \Phi(s)^{-1} e_i \quad \text{for} \quad s \neq 0. \end{aligned}$$

Here, by using the index i, we emphasize that it is the transfer function from agent i to MAS according to Problem 1. From the definition of the function Φ given by Eq. (7) and $LVV^\top = L$, for $s \neq 0$ we obtain that

$$\Phi(s) = -s^2 I + \mathrm{i}s(\beta I + \alpha L) + \gamma L.$$

Note that $\Phi(0) = \gamma L$ is not invertible. In order to obtain a formula for the transfer function in zero, we will additionally analyze this case.

In order to determine $F_i(0) = \tilde{C}(-\tilde{A})^{-1}\tilde{B}_i$, we first calculate the inverse of matrix $-\tilde{A}$. We calculate blocks of the matrix $(-\tilde{A})^{-1} = \begin{bmatrix} A_{11} & A_{12} \\ A_{21} & A_{22} \end{bmatrix}$ using the equations:

$$\begin{bmatrix} A_{11} & A_{12} \\ A_{21} & A_{22} \end{bmatrix}\begin{bmatrix} 0 & -V^T \\ \gamma LV & \beta I + \alpha L \end{bmatrix} = I,$$

$$\begin{bmatrix} 0 & -V^T \\ \gamma LV & \beta I + \alpha L \end{bmatrix}\begin{bmatrix} A_{11} & A_{12} \\ A_{21} & A_{22} \end{bmatrix} = I.$$

Considering the corresponding blocks, we obtain the following equations:

$$\gamma A_{12} LV = I, \tag{8}$$

$$-A_{11}V^T + A_{12}(\beta I + \alpha L) = 0, \tag{9}$$

$$\gamma A_{22} LV = 0, \tag{10}$$

$$-A_{21}V^T + A_{22}(\beta I + \alpha L) = I, \tag{11}$$

$$-V^T A_{21} = I, \tag{12}$$

$$-V^T A_{22} = 0, \tag{13}$$

$$\gamma LVA_{11} + (\beta I + \alpha L)A_{21} = 0, \tag{14}$$

$$\gamma LVA_{12} + (\beta I + \alpha L)A_{22} = I. \tag{15}$$

Eqs. (10) and (13) are satisfied when $A_{22} = 0$. Now, from Eq. (11) using that $V^\top V = I$, we obtain $-A_{21}V^\top = I \Rightarrow A_{21} = -V$ and the Eq. (12) is immediately satisfied.

Now, from Eqs. (8) and (15) we have conditions for A_{12}:

$$\gamma A_{12} L V = I,$$
$$\gamma L V A_{12} = I.$$

From the latter equation, we have $\gamma V^\top L V A_{12} = V^\top \Rightarrow A_{12} = \frac{1}{\gamma}(V^\top L V)^{-1} V^\top$, which satisfies the first equation as well.

Now, using the obtained formula for A_{12} and Eq. (9), it follows that

$$A_{11} = \frac{1}{\gamma}(V^\top L V)^{-1} V^\top (\beta I + \alpha L) V.$$

From $L = LVV^\top$, we obtain that the Eq. (14) is also satisfied. Finally, we reach

$$\begin{aligned} F_i(0) &= \begin{bmatrix} V & 0 \end{bmatrix} \begin{bmatrix} \frac{1}{\gamma}(V^\top L V)^{-1} V^\top (\beta I + \alpha L) V & \frac{1}{\gamma}(V^\top L V)^{-1} V^\top \\ -V & 0 \end{bmatrix} \begin{bmatrix} 0 \\ e_i \end{bmatrix} \\ &= \frac{1}{\gamma} V (V^\top L V)^{-1} V^\top e_i. \end{aligned} \tag{16}$$

Note that

$$F_i(0) = \frac{1}{\gamma} L^+ e_i, \tag{17}$$

where L^+ is the Moore-Penrose pseudoinverse of L.

Recall that the H_∞ norms of F_i's are what we are interested in as they measure the ith agent disturbance impact on the entire system. To harmonize the $F_i(s)$ expressions for all s, note that we can write

$$\Phi(s) = (\mathrm{i}s\alpha + \gamma)\left(\frac{-s^2 + \mathrm{i}s\beta}{\gamma + \mathrm{i}s\alpha} I + L\right).$$

Hence, we have

$$F_i(s) = \frac{1}{\gamma + \mathrm{i}s\alpha} V V^T (L - \mu(s) I)^{-1} e_i, \tag{18}$$

with

$$\mu(s) = \frac{s^2 - \mathrm{i}s\beta}{\gamma + \mathrm{i}s\alpha}.$$

Since $VV^\top$ is the orthogonal projection to the orthogonal complement of the subspace spanned by the vector $\mathbf{1}$, we know that $VV^\top = I - n^{-1}\mathbf{1}\mathbf{1}^\top$ and hence $VV^\top L^+ = L^+$. This implies that for all s we can write

$$F_i(s) = \frac{1}{\gamma + \mathrm{i}s\alpha} V V^T (L - \mu(s) I)^{+} e_i.$$

Observe that the H_∞ norm of the transfer function F_i is

$$\|F_i\|_\infty^2 = \sup_s \|F_i(s)\|_2^2 = \sup_s \frac{1}{\gamma^2 + s^2\alpha^2} \|VV^\top (L - \mu(s) I)^{+} e_i\|_2^2.$$

Hence, the calculation of $\|F_i\|_\infty$ boils down to finding the maximum of the function $\mathbb{R} \ni s \mapsto \frac{1}{\sqrt{\gamma^2+s^2\alpha^2}}\|VV^\top(L-\mu(s)I)^+e_i\|$. To achieve this, the main computation cost is solving linear systems $(L-\mu(s)I)x = e_i$ for a sequence of choices of s given by the optimization method in use.

Before moving to the main result of this article, let us point out the following (minor) contribution of the present work. Namely, in comparison with the model reduction from Tolić [36], which leverages the Real Jordan Form, the aforestated MAS model reduction is more scalable and numerically stable. For example, the methodology from Tolić [36] is struggling numerically even with MASs containing about 20 agents (i.e., the model reduction takes several hours to complete).

4.2. Main result

In the proof of Theorem 1, we use the following result

Lemma 1 ([40], Corollary 4.5.11)**.** *Let $A, S \in \mathbb{R}^{n\times n}$ and let A be a Hermitian matrix. Let the eigenvalues of A and SS^* be arranged in increasing order. For each $k = 1, \dots, n$ there exists a nonnegative real number θ_k such that $\lambda_1(SS^*) \le \theta_k \le \lambda_n(SS^*)$ and $\lambda_k(SAS^*) = \theta_k\lambda_k(A)$.*

Theorem 1. *Suppose that ($\gamma \le \alpha\beta$) or ($\gamma > \alpha\beta$ and $\|L\| \le \frac{\beta^2}{2(\gamma-\alpha\beta)}$). Then for all $i \in \{1, \dots, n\}$ we have*

$$\|F_i\|_\infty = \|F_i(0)\|_2.$$

Proof. We assume that columns of V are eigenvectors of L that correspond to the non-zero eigenvalues. Let $\hat{V} = [\mathbf{1}\ V] \in \mathbb{R}^{n\times n}$. Then $L = \hat{V}\Lambda\hat{V}^\top$, where $\Lambda = \operatorname{diag}(\lambda_1, \lambda_2, \dots, \lambda_n) = \operatorname{diag}(0, \lambda_2, \dots, \lambda_n)$. Note that $V^\top\hat{V} = [0\ I_{n-1}]$. We denote $\Lambda_2 = \operatorname{diag}(\lambda_2, \dots, \lambda_n)$. Using Eq. (18), from

$$\begin{aligned} F_{ij}(s) :&= e_j^\top F_i(s) = e_j^\top VV^\top\Phi(s)^{-1}e_i = \frac{1}{\gamma+\mathrm{i}s\alpha}e_j^\top VV^\top(L-\mu(s))^{-1}e_i \\ &= \frac{1}{\gamma+\mathrm{i}s\alpha}e_j^\top[0\ V](\Lambda-\mu(s))^{-1}\hat{V}^\top e_i = \frac{1}{\gamma+\mathrm{i}s\alpha}e_j^\top V(\Lambda_2-\mu(s))^{-1}V^\top e_i \end{aligned} \tag{19}$$

we obtain

$$\begin{aligned} |F_{ij}(s)|^2 &= \frac{1}{\gamma^2+s^2\alpha^2}e_j^\top V(\Lambda_2-\mu(s))^{-1}V^\top e_ie_i^\top V\left(\Lambda_2-\overline{\mu(s)}\right)^{-1}V^\top e_j \\ &= \frac{1}{\gamma^2+s^2\alpha^2}e_j^\top V\left(I-\mu(s)\Lambda_2^{-1}\right)^{-1}\Lambda_2^{-1}V^\top e_ie_i^\top V\Lambda_2^{-1}\left(I-\overline{\mu(s)}\Lambda_2^{-1}\right)^{-1}V^\top e_j \\ &= \frac{1}{\gamma^2+s^2\alpha^2}e_j^\top V(s)QV(s)^*e_j, \end{aligned}$$

with $V(s) = V(I-\mu(s)\Lambda_2^{-1})^{-1} \in \mathbb{C}^{n\times(n-1)}$ and $Q = \Lambda_2^{-1}V^\top e_ie_i^\top V\Lambda_2^{-1} \in \mathbb{R}^{(n-1)\times(n-1)}$.

Note that from Eq. (19) we obtain

$$F_{ij}(0) = \frac{1}{\gamma}e_j^\top V\Lambda_2^{-1}V^\top e_i = \frac{1}{\gamma}e_j^\top\hat{V}\begin{bmatrix}0 & 0\\ 0 & \Lambda_2^{-1}\end{bmatrix}\hat{V}^\top e_i = \frac{1}{\gamma}e_j^\top L^+e_i.$$

Let $\hat{V}(s) = [0\ V(s)] \in \mathbb{C}^{n\times n}$ and $\hat{Q} = \begin{bmatrix} 0 & 0 \\ 0 & Q \end{bmatrix} \in \mathbb{R}^{n\times n}$. Then $V(s)QV(s)^* = \hat{V}(s)\hat{Q}\hat{V}(s)^*$. Next, we calculate

$$\begin{aligned}\hat{V}(s)\hat{V}(s)^* = V(s)V(s)^* &= V\big(I-\mu(s)\Lambda_2^{-1}\big)^{-1}\Big(I-\overline{\mu(s)}\Lambda_2^{-1}\Big)^{-1}V^\top \\ &= V\ \mathrm{diag}\left(\frac{1}{(1-\Re\mu(s)\lambda_k^{-1})^2+(\Im\mu(s))^2\lambda_k^{-2}} : k=2,\dots,n\right)V^\top \\ &= V\ \mathrm{diag}\left(\frac{\lambda_k^2}{\lambda_k^2-2\lambda_k\Re(\mu(s))+|\mu(s)|^2} : k=2,\dots,n\right)V^\top.\end{aligned}$$

This implies that the singular values of $\hat{V}(s)$ are given by

$$\sigma_k(s) = \frac{\lambda_k^2}{\lambda_k^2-2\lambda_k\Re(\mu(s))+|\mu(s)|^2}$$

for $k=2,\dots,n$. To be able to apply Lemma 1 and obtain the desired inequality $\lambda_n(\hat{V}(s)\hat{Q}\hat{V}(s)^*) \le \lambda_n(\hat{Q})$, we need to ensure that $0 \le \sigma_k(s) \le 1$. Thus, we need to ensure $|\mu(s)|^2 - 2\lambda_k\Re(\mu(s)) \ge 0$ for all $k=2,\dots,n$. Taking into account the definition of $\mu(s)$, we obtain the following inequality

$$2\lambda_k(\gamma-\alpha\beta) \le s^2+\beta^2.$$

If $\gamma \le \alpha\beta$, this inequality is obviously always satisfied. If, on the other hand, $\gamma > \alpha\beta$, we obtain $\lambda_k \le \frac{s^2+\beta^2}{2(\gamma-\alpha\beta)}$. To ensure that this inequality is satisfied for all $s>0$ and $k=2,\dots,n$, we arrive at the assumption $\|L\| \le \frac{\beta^2}{2(\gamma-\alpha\beta)}$.

We now apply Lemma 1 with $S=\hat{V}(s)$ and $A=\hat{Q}$ and obtain that for all $s>0$ there exist numbers $\theta(s)$ such that $0\le\theta(s)\le 1$ and $\lambda_n(V(s)QV(s)^*) = \theta(s)\lambda_n(\hat{Q})$, where $\lambda_n(M)$ denotes the largest eigenvalue of the matrix M. As $V(s)QV(s)^*$ is a rank one matrix, we obtain

$$\begin{aligned}\lambda_n(V(s)QV(s)^*) &= \|V(\Lambda_2-\mu(s)I)^{-1}V^\top e_i\|^2 = \sum_{j=1}^{n}|e_j^\top V(\Lambda_2-\mu(s)I)^{-1}V^\top e_i|^2 \\ &= \big(\gamma^2+s^2\alpha^2\big)\|F_i(s)\|^2\end{aligned}$$

and $\lambda_n(\hat{Q}) = \|\Lambda_2^{-1}V^\top e_i\|^2$. As $F_i(s)=0$ would imply $(L-\mu(s)I)\mathbf{1}=e_i$, which is not true, it follows that $\theta(s)>0$ for all $s>0$. Since

$$\|\Lambda_2^{-1}V^\top e_i\|^2 = \|V^\top V\Lambda_2^{-1}V^\top e_i\|^2 \le \|V\Lambda_2^{-1}V^\top e_i\|^2 = \lambda_n\big(V(0)QV(0)^\top\big)$$

and

$$V(0)QV(0)^\top = V\Lambda_2^{-1}V^\top e_ie_i^\top V\Lambda_2^{-1}V^\top = \|L^+e_i\|^2,$$

we finally obtain

$$\|F_i(s)\|^2 \le \frac{\gamma^2}{\gamma^2+s^2\alpha^2}\theta(s)\|F_i(0)\|^2.$$

From $0<\frac{\gamma^2}{\gamma^2+s^2\alpha^2}\theta(s)<1$ for all $s>0$, the statement of the theorem follows. □

Remark 1. The first condition of the above theorem boils down to $c_1 \leq T_s c_2$, which is somewhat concerning as it requires the position feedback gain c_1 to be typically smaller than the velocity feedback gain c_2, which is often undesirable in practice owing to velocity measurements being more noisy than position measurements, especially at high frequency ranges [37,38]. Namely, being velocity integrals, positions smooth out velocity noise making them less wiggly. On the other hand, since our problem settings do not involve modeling uncertainties nor noisy measurements, the obtained theoretical result is not surprising in light of the low-pass filter discussion from the introductory section as confirmed by Section 5. Nevertheless, this real-life applicability observation warrants the experimental verification of Section 6 to examine robustness of Problem 1 and Theorem 1.

Remark 2. From Theorem 1 it follows that under its assumptions, one can calculate the H_∞ norm of agent-to-system using

$$\|F_i\|_\infty^2 = \frac{1}{\gamma^2}\sum_{j=1}^{n}(L_{ij}^+)^2 = \frac{1}{\gamma^2}\|L^+ e_i\|^2. \tag{20}$$

Hence, under the assumptions of Theorem 1, the main computational cost in calculating $\|F_i\|_\infty$ *for all agents* i is to calculate the pseudoinverse of the matrix L. As illustrated in Section 5, this is obviously several orders of magnitude faster then calculating $\|F_i\|_\infty$ by a general algorithm for the H_∞ norm. This allows us to efficiently rank all agents of the system according to their corresponding H_∞ norm.

Also note that we have $\|F_i\|_\infty \geq \sqrt{2L_{ii}^+}$; hence, from the diagonal of L^+ one can estimate the H_∞ norm of systems. Since the pseudoinverse of a graph Laplacian and its diagonal are important objects of study in various disciplines, there is a wealth of literature covering their efficient computation and/or approximation schemes (see, for example, [41,42] and [43]). In this article, we do not pursue this line of research, but it is clear that the use of such methods would further increase the efficiency of our method.

Remark 3. The efficient calculation of the H_∞ norm allows one to calculate the impact of all the agents on the system. This can be used to provide directions towards improving communication graph design and tuning/selecting cooperative control mechanisms. For example, from Fig. 2 one can see that if one wants to improve the spread of information, the existence of large clusters of agents is not desirable.

From the proof of Theorem 1 it follows that for systems which do not attain the H_∞ norm in zero, one must have $\lambda_2 > \frac{\beta^2}{2(\gamma-\alpha\beta)}$, i.e., the Fiedler value (also called the algebraic connectivity) has to be larger than a certain constant, which only depends on the parameters of the system and not the geometry of MAS. Obviously, this is only a necessary condition. In Example 3, we give a MAS that violates the assumptions of Theorem 1 and for which the H_∞ norm is not attained at zero. Also, from Example 2 it is clear that the statement of Theorem 1 does not hold when calculating the H_∞ norm of the influence between two agents.

Remark 4. The property $\|G\|_\infty = \overline{\sigma}(G(0))$ is well-known to hold for positive systems [44], but the systems we are studying, in general, do not satisfy this property.

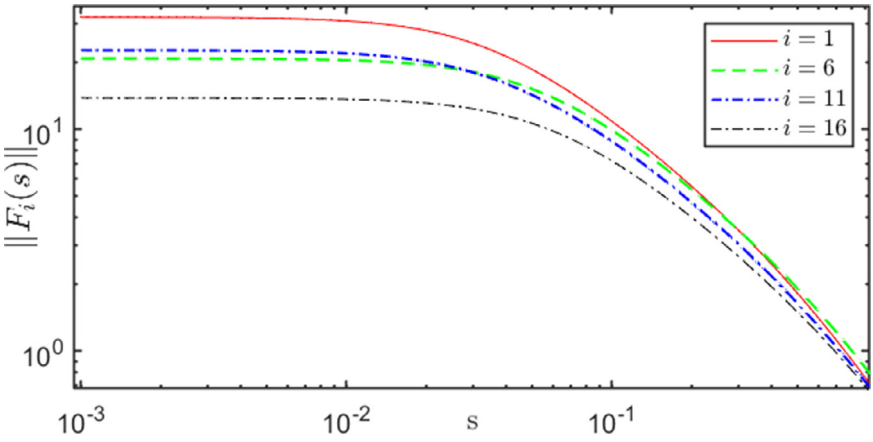

Fig. 1. Transfer functions for Example 1.

5. Numerical examples

Example 1. First we illustrate our main result given by Theorem 1. The matrix L is the graph Laplacian illustrated in Fig. 2 and the matrix L itself can be downloaded at [45]. For the illustration purposes, we consider here just dimension $n = 20$, while later in this section we show computational benefits of our result. Following the notation from Section 3, we select the following system parameters $K_s = 5.2$, $T_s = 0.38$, $K = 0.5$, $c_1 = 0.05$ and $c_2 = 0.5$ motivated by the MAS experiments in [37]. Since $\gamma - \alpha\beta = -0.364 < 0$, the first assumption of Theorem 1 is satisfied. In Fig. 1 we show transfer functions defined by Eq. (18) for several different agents i that determine the input matrix B_i from Eq. (4). In particular, on the x-axis we have the frequency s^{-1}, while the y-axis shows the magnitude of $F_i(s)$ for four different agents i. Employing Eq. (20), this figure illustrates the influence of different agents i on the H_∞ norm of the system, but it also shows that the H_∞ norm is attained at zero frequency.

Fig. 2 illustrates the relative importance of agents; the radius of the ith node is proportional to $\|F_i\|_\infty$. Also the thickness of each edge is proportional to the corresponding edge weight. As can be seen, the "hubs" of the MAS aren't the most influential agents. The ordering seems to be related to the ordering obtained by using the so-called topological centrality of nodes [46], which can also be calculated using the pseudoinverse of the graph Laplacian, but it does not coincide with it. It seems that the most influential nodes are those which belong to the largest number of spanning trees.

Example 2. This example considers the same configuration presented in the previous example, but here we consider the impact of the ith agent to the jth agent. This means that the output matrix is given by $C_j = \begin{bmatrix} e_i & \mathbf{0}_n^\top \end{bmatrix}^\top$. Here we would like to illustrate that in this case the H_∞ norm is not attained at zero, even though the assumptions of Theorem 1 hold. Hence, the theorem cannot be extended to cover the agent-to-agent influence. In particular, this implies that the systems $(\tilde{C}, \tilde{A}, [0\ I]^\top)$ are, in general, not positively dominated [44]. Fig. 3 shows the transfer function for different pairs (i, j). The y-axis shows the magnitude of the transfer function $\|F_{ij}(s)\|_\infty$ for four different pairs of (i, j), where the index i determines the input matrix B_i and the index j determines the output matrix C_j.

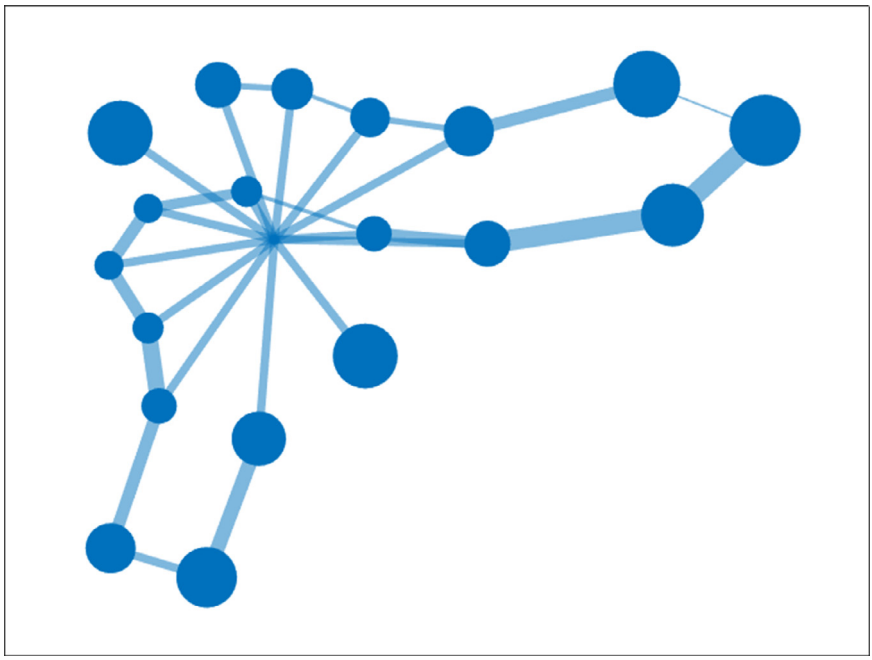

Fig. 2. Agents' importance in Example 1. The radius of the ith node is proportional to $\|F_i\|_\infty$ and the thickness of each edge is proportional to the corresponding edge weight.

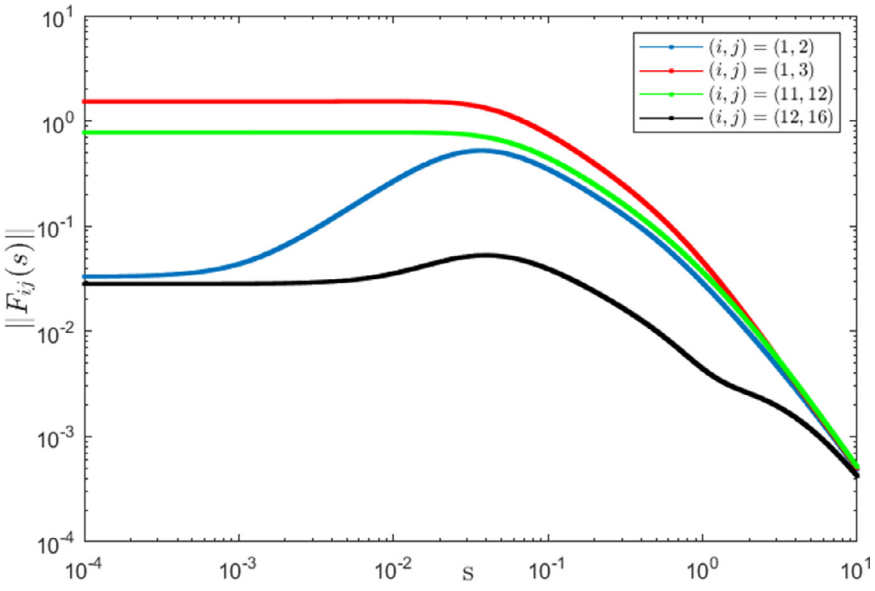

Fig. 3. Transfer functions in Example 2.

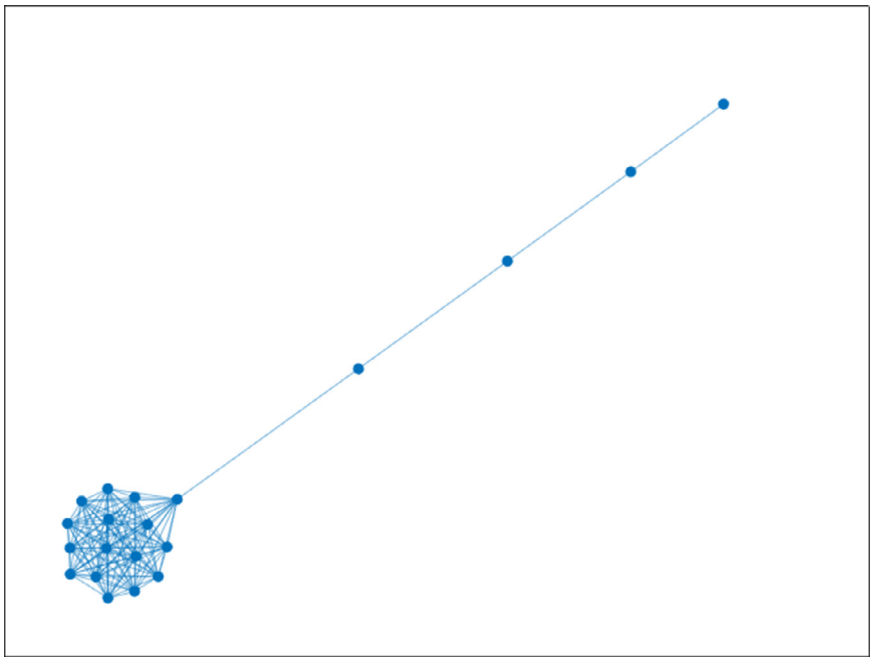

Fig. 4. Graph associated with Example 3.

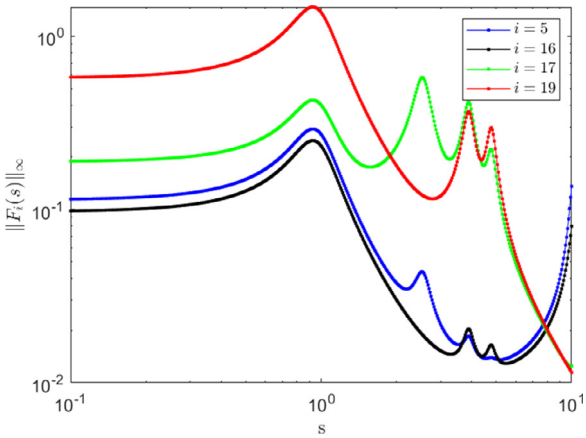

Fig. 5. Transfer functions for Example 3 in which the conditions of the main theorem are not met.

Example 3. Let us consider the 'lollipop' graph with $n = 20$ (for more about the 'lollipop' graphs, see [47]). The utilized matrix L can be downloaded at [45]. Here we show that if the assumptions of Theorem 1 do not hold, then the maximum of our transfer function Eq. (18) need not be attained at zero. The Laplacian matrix L (that is, the underlying graph) is illustrated in Fig. 4. We consider the following system parameters: $K_s = 5.2$, $T_s = 0.38$, $K = 0.5$, $c_1 = 2.5$ and $c_2 = 0.005$. Now, $\gamma - \alpha\beta = 6.4951 > 0$ and $\|L\| - \frac{\beta^2}{2(\gamma-\alpha\beta)} = 16.993 > 0$, which means that the assumptions of Theorem 1 are not satisfied. From the Fig. 5, it is

Table 1
Runtime comparison.

n	using formula Eq. (20)	MATLAB function `hinfnorm`
250	0.007 s	7.806 min
10,000	5.55 min	n/a

obvious that the maximum is not attained at zero and this additionally testifies sharpness of the bounds in our main result.

Example 4. The last example is similar to Example 3, but here $c_1 = 0.05$, $c_2 = 0.5$ and now we consider a significantly larger number of agents n to illustrate the computational benefits of our approach. In particular, two different dimensions n are considered. Table 1 shows the total time needed for calculation of $\|F_i\|_\infty$, $\forall i = 1, 2, \ldots, n$. In our case, we use the formula Eq. (20) whilst the standard approach in MATLAB is to use the function `hinfnorm` (with tolerance 0.001). Since that standard calculation of the H_∞ norm is demanding even for moderate dimensions, calculations with MATLAB's function `hinfnorm` for $n = 10000$ are not feasible. Note the huge difference in the calculation time for $n = 250$ of our approach and of the standard approach via the MATLAB's function. Furthermore, our formula for $n = 10000$ is even faster than the MATLAB's for $n = 250$. The graph Laplacians used in the example can be downloaded at [45].

These computations were carried out on a machine with an Intel® Core™ processor i7 − 1165G CPUs and 16 GB RAM. The MATLAB results are calculated by the MATLAB version 9.8.0.1323502 (R2020a) on a 64-bit Windows operating system.

6. Experimental results

An in-detail description of our testbed comprised of low-cost components including HTC Vive Lighthouse stations and Bitcraze Lighthouse positioning decks mounted on four Crazyflie nano quadrotors can be found in [38]. The system identification performed in [38] yields parameters $K_s = 0.95$ and $T_s = 0.45$ in (1). Notice that the time delay (that is, dead time) of 0.45s from [38] is approximated by T_s owing to the first-order Padé approximation. In addition, the output feedback constants in Eq. (2) are selected as $c_1 = 0.1$ and $c_2 = 1$ whereas the controller gain is $K = 0.45$. Clearly, the $\gamma \leq \alpha\beta$ condition of Theorem 1 is fulfilled. Furthermore, the control loop sampling frequency is 40Hz whilst the topology is given by

$$L = \begin{bmatrix} 1 & 0 & -1 & 0 \\ 0 & 2 & -1 & -1 \\ -1 & -1 & 3 & -1 \\ 0 & -1 & -1 & 2 \end{bmatrix}. \tag{21}$$

The team is disturbed through the first agent with the sinusoidal signal of amplitude 0.1m and period 1.5rad/s. Subsequently, the constant disturbance value -0.02m/s^2 is applied at the first agent as well. The obtained signals are provided in Fig. 6 whereas their spectra are in Fig. 7.

The first plot in Fig. 6 illustrates the existence of unaccounted for disturbances (e.g., modeling uncertainties, inter-agent interference, coupling among agents' control loops, etc.) and noisy measurements. We measure the impact of these unaccounted for phenomena using the $\mathcal{L}_2$-norm of $\|\chi\|$ w.r.t. consensus manifold normalized over time and obtain 0.0096. Since

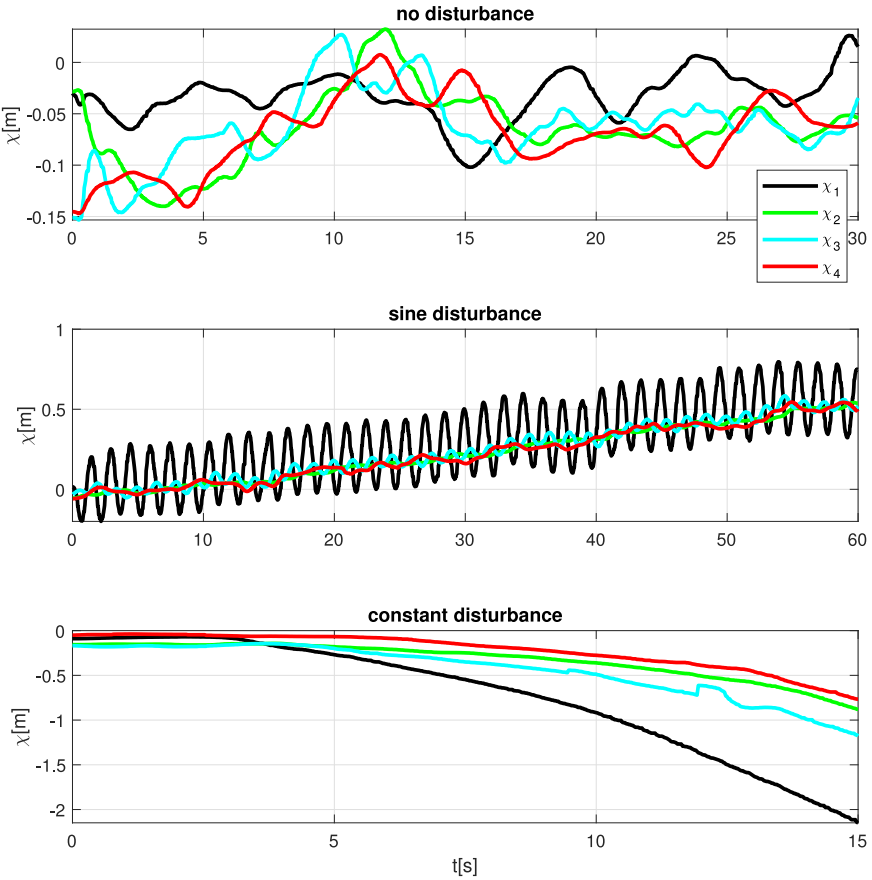

Fig. 6. Experimentally obtained signals.

we cannot measure the $\mathcal{L}_2$-norm of the inherent disturbances, we cannot infer much about the associated H_∞-norm. In what follows, we assume that the level of inherent disturbances is negligible in comparison with the user-imposed disturbances. Since in the remaining two plots of Fig. 6, where the disturbances are imposed onto the first agent, it is straightforward to estimate the corresponding H_∞ norm as the ratio of the $\mathcal{L}_2$-norms of outputs and applied inputs. This way of obtaining/estimating the H_∞ norm comes from nonlinear systems [36], where the modes of input signals do not necessarily excite only the same modes in the outputs (as seen from the second plot in Fig. 7). The obtained H_∞ norm for the sinusoidal input is 2.2043 while for the constant input is 25.9579. Clearly, the impact of the constant disturbance is much greater than the impact of the sinusoidal disturbance, which verifies Theorem 1.

The first plot in Fig. 7 presents the spectrum of $\|\chi(t)\|$ w.r.t. consensus manifold obtained when the MAS is "at rest". Of course, the system is not really at rest owing to the inherent realistic phenomena, but that is as close as we can get to the no-disturbance settings. It is worth mentioning that all spectra are obtained using the Fast Fourier Transformation (FFT). The second plot shows several low-frequency harmonics excited by the sinusoidal input (since the MAS is in fact nonlinear). It is to be pointed out that sines with various frequencies and

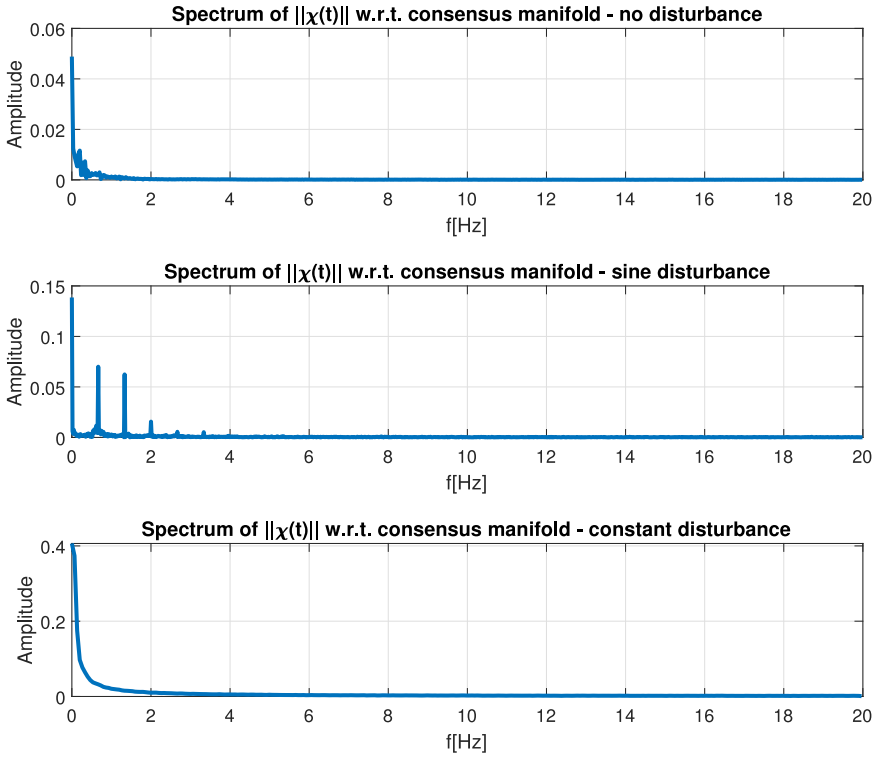

Fig. 7. Amplitude spectra of signals of interest obtained via FFT.

amplitudes were applied all with similar outcomes and hence are not enclosed herein for brevity. The last plot in Fig. 7 provides a clear evidence that constant inputs affect our MAS more than signals at other frequencies and that the greatest impact is on the zero frequency component of output. All plots in Fig. 7 show that our concerns regarding the high-frequency noises potentially present in experiments were not justified. We presume that the relatively high sampling rate of 40Hz, as opposed to the intermittent data exchange from [38], is behind this reassuring observation. Altogether, these experiments attest a certain robustness level present in our problem setting and conditions of Theorem 1.

7. Conclusions

This article presents sufficient conditions that greatly improve agent-to-system H_∞ norm computations in MASs. Undirected weighted topologies and second-order linear homogeneous agent dynamics are considered. The presented theoretical results are successfully verified experimentally in a rather challenging disturbance and noise setting.

The future research avenues include H_2 norm analyses, directed and time-varying topologies as well as more general MASs including heterogeneous agents with higher order dynamics. Lastly, a more formal and theoretical investigation of realistic phenomena present in MASs is in order.

Declaration of Competing Interest

The authors declare that they have no known competing financial interests or personal relationships that could have appeared to influence the work reported in this paper.

CRediT authorship contribution statement

Ivica Nakić: Conceptualization, Methodology, Formal analysis, Validation, Writing – original draft. **Domagoj Tolić:** Conceptualization, Methodology, Software, Validation, Investigation, Writing – original draft, Visualization. **Zoran Tomljanović:** Conceptualization, Methodology, Formal analysis, Software, Investigation, Validation, Writing – original draft, Visualization. **Ivana Palunko:** Conceptualization, Methodology, Validation, Investigation, Resources, Writing – original draft.

References

[1] W. Ren, R.W. Beard, Distributed Consensus in Multi-Vehicle Cooperative Control - Theory and Applications, Communications and Control Engineering, Springer, London, 2008.
[2] D. Tolić, V. Jeličić, V. Bilas, Resource management in cooperative multi-agent networks through self-triggering, IET Control Theory Appl. 9 (13) (2015) 915–928.
[3] Z. Tomljanović, M. Voigt, Semi-active $\mathcal{H}_\infty$-norm damping optimization by adaptive interpolation, Numer. Linear Algebra Appl. 27 (4) (2020) 1–17.
[4] I. Nakić, Z. Tomljanović, N. Truhar, Mixed control of vibrational systems, J. Appl. Math. Mech. 99 (9) (2019) 1–15.
[5] K. Veselić, Damped Oscillations of Linear Systems, Springer Lecture Notes in Mathematics, Springer-Verlag, Berlin, 2011.
[6] S.L. (Eds.), Social Networks. A Developing Paradigm, Academic Press, 1977.
[7] B. Zhao, Y.K. Li, J.C.S. Lui, D.M. Chiu, Mathematical modeling of advertisement and influence spread in social networks, in: ACM Workshop on the Economics of Networked Systems (NetEcon), 2009.
[8] A.V. Proskurnikov, R. Tempo, A tutorial on modeling and analysis of dynamic social networks. Part I, Annu. Rev. Control 43 (2017) 65–79.
[9] S. Peng, Y. Zhou, L. Cao, S. Yu, J. Niu, W. Jia, Influence analysis in social networks: a survey, J. Netw. Comput. Appl. 106 (2018) 17–32.
[10] F. Sorrentino, D. Tolić, R. Fierro, S. Picozzi, J.R. Gordon, A. Mammoli, Stability analysis of a model for the market dynamics of a smart grid, in: 52nd IEEE Conference on Decision and Control, 2013, pp. 4964–4970.
[11] G. Dileep, A survey on smart grid technologies and applications, Renew. Energy 146 (2020) 2589–2625.
[12] K. Zhou, J.C. Doyle, K. K Glover, Robust and Optimal Control, Prentice Hall, Upper Saddle River, NJ, 1996.
[13] S. Boyd, V. Balakrishnan, A regularity result for the singular values of a transfer matrix and a quadratically convergent algorithm for computing its $\mathcal{L}_\infty$-norm, Syst. Control Lett. 15 (1) (1990) 1–7.
[14] N. Aliyev, P. Benner, E. Mengi, P. Schwerdtner, M. Voigt, A greedy subspace method for computing the $\mathcal{L}_\infty$-norm, PAMM Proc. Appl. Math. Mech. 17 (1) (2017) 751–752.
[15] Y. Chahlaoui, K. Gallivan, P. Van Dooren, $\mathcal{H}_\infty$-norm calculations of large sparse systems, in: Proc. Internat. Symposium Math. Theory Networks Syst., 2004. Leuven, Belgium
[16] P. Benner, V. Sima, M. Voigt, $\mathcal{L}_\infty$-norm computation for continuous-time descriptor systems using structured matrix pencils, IEEE Trans. Automat. Control 57 (1) (2012) 233–238.
[17] N. Guglielmi, M. Gürbüzbalaban, M.L. Overton, Fast approximation of the H_∞ norm via optimization over spectral value sets, SIAM J. Matrix Anal. Appl. 34 (2) (2013) 709–737.
[18] T. Mitchell, M.L. Overton, Hybrid expansion-contraction: a robust scaleable method for approximating the H_∞ norm, IMA J. Numer. Anal. 36 (3) (2016) 985–1014.
[19] L. Bao, J.J. Garcia-Luna-Aceves, Link-state routing in networks with unidirectional links, in: Proceedings Eight International Conference on Computer Communications and Networks (Cat. No.99EX370), 1999, pp. 358–363.
[20] V.V. Dimakopoulos, E. Pitoura, A peer-to-peer approach to resource discovery in multi-agent systems, in: M. Klusch, A. Omicini, S. Ossowski, H. Laamanen (Eds.), Cooperative Information Agents VII, Springer-Verlag, Berlin, Heidelberg, 2003, pp. 62–77.

[21] I. Saboori, K. Khorasani, H_∞ consensus achievement of multi-agent systems with directed and switching topology networks, IEEE Trans. Automat. Control 59 (11) (2014) 3104–3109.
[22] A. Elahi, A. Alfi, H. Modares, H_∞ consensus control of discrete-time multi-agent systems under network imperfections and external disturbance, IEEE/CAA J. Autom. Sin. 6 (3) (2019) 667–675.
[23] F.A. Yaghmaie, K.H. Movrić, F.L. Lewis, R. Su, Differential graphical games for H_∞ control of linear heterogeneous multiagent systems, Int. J. Robust Nonlinear Control 29 (10) (2019) 2995–3013.
[24] A.A. Stoorvogel, A. Saberi, M. Zhang, Z. Liu, Solvability conditions and design for H_∞ & H_2 almost state synchronization of homogeneous multi-agent systems, Eur. J. Control 46 (2019) 36–48.
[25] Z. Li, Z. Duan, L. Huang, H_∞ control of networked multi-agent systems, J. Syst. Sci. Complexity 29 (1) (2009) 35–48.
[26] X. Li, Y.-C. Soh, L. Xie, Robust consensus of uncertain linear multi-agent systems via dynamic output feedback, Automatica 98 (2018) 114–123.
[27] G. Wen, T. Huang, W. Yu, Y. Xia, Z.-W. Liu, Cooperative tracking of networked agents with a high-dimensional leader: qualitative analysis and performance evaluation, IEEE Trans. Cybern. 48 (7) (2018) 2060–2073.
[28] D. Nojavanzadeh, Z. Liu, A. Saberi, A.A. Stoorvogel, H_∞ and H_2 almost output and regulated output synchronization of heterogeneous multi-agent systems: ascale-free protocol design, J. Franklin Inst. 358 (18) (2021) 9841–9866.
[29] Y. Chengzhi, I. Shahab, Z. Wei, H_∞ output containment control of heterogeneous multi-agent systems via distributed dynamic output feedback, J. Franklin Inst. 355 (12) (2018) 5058–5081.
[30] H. Fei, W. Guoliang, D. Dedui, S. Yan, Finite-horizon H_∞-consensus control for multi-agent systems with random parameters: the local condition case, J. Franklin Inst. 354 (14) (2017) 6078–6097.
[31] J. Han, H. Zhang, H. Jiang, Event-based H_∞ consensus control for second-order leader-following multi-agent systems, J. Franklin Inst. 353 (18) (2016) 5081–5098.
[32] Y. Sun, P. Shi, C.-C. Lim, Event-triggered sliding mode scaled consensus control for multi-agent systems, J. Franklin Inst. 359 (2) (2022) 981–998.
[33] J. Wang, Z. Duan, Y. Zhao, G. Qin, Y. Yan, H_∞ and H_2 control of multi-agent systems with transient performance improvement, Int. J. Control 86 (12) (2013) 2131–2145.
[34] G.E. Dullerud, F. Paganini, A Course in Robust Control Theory: A Convex Approach, Vol. 36, Springer Science & Business Media, 2013.
[35] R. Olfati-Saber, R.M. Murray, Consensus problems in networks of agents with switching topology and time-delays, IEEE Trans. Autom. Control 49 (9) (2004) 1520–1533.
[36] D. Tolić, Lp-stability with respect to sets applied towards self-triggered communication for single-integrator consensus, in: 52nd IEEE Conference on Decision and Control, 2013, pp. 3409–3414.
[37] D. Tolić, I. Palunko, A. Ivanović, M. Car, S. Bogdan, Multi-agent control in degraded communication environments, in: 2015 European Control Conference (ECC), 2015, pp. 404–409.
[38] I. Palunko, D. Tolić, V. Prkačin, Learning near-optimal broadcasting intervals in decentralized multi-agent systems using online least-square policy iteration, IET Control Theory Appl. 15 (8) (2021) 1054–1067.
[39] D. Kingston, W. Ren, R. Beard, Consensus algorithms are input-to-state stable, in: Proceedings of the 2005, American Control Conference, 2005., 2005, pp. 1686–1690 vol. 3.
[40] R.A. Horn, C.R. Johnson, Matrix Analysis, Cambridge University Press, 2012.
[41] G. Ranjan, Z.-L. Zhang, D. Boley, Incremental computation of pseudo-inverse of Laplacian, in: International Conference on Combinatorial Optimization and Applications, Springer, 2014, pp. 729–749.
[42] A. Jambulapati, A. Sidford, Efficient $\widetilde{O}(n/\epsilon)$ spectral sketches for the Laplacian and its pseudoinverse, in: Proceedings of the Twenty-Ninth Annual ACM-SIAM Symposium on Discrete Algorithms, SIAM, 2018, pp. 2487–2503.
[43] E. Angriman, M. Predari, A. van der Grinten, H. Meyerhenke, Approximation of the diagonal of a Laplacian's pseudoinverse for complex network analysis, in: 28th Annual European Symposium on Algorithms (ESA 2020), Schloss Dagstuhl-Leibniz-Zentrum für Informatik, 2020.
[44] A. Rantzer, Distributed control of positive systems, in: 2011 50th IEEE Conference on Decision and Control and European Control Conference, IEEE, 2011, pp. 6608–6611.
[45] I. Nakić, D. Tolić, Z. Tomljanović, I. Palunko, Numerically efficient H_∞ analysis of cooperative multi-agent systems: dataset, 2021, 10.5281/zenodo.5531365
[46] G. Ranjan, Z.-L. Zhang, Geometry of complex networks and topological centrality, Physica A 392 (17) (2013) 3833–3845.
[47] J. Jonasson, Lollipop graphs are extremal for commute times, Random Struct. Algorithms 16 (2) (2000) 131–142.